

Unsaturated-Compound Hydrogenation Nanocatalysts Based on Palladium and Platinum Particles Immobilized in Pores of Mesoporous Aromatic Frameworks

L. A. Kulikov, M. V. Terenina, I. Yu. Kryazheva, and E. A. Karakhanov*

Faculty of Chemistry, Moscow State University, Moscow, Russia

**e-mail: kar@petrol.chem.msu.ru*

Received September 29, 2016

Abstract—Heterogeneous catalysts for the hydrogenation of unsaturated hydrocarbons have been synthesized on the basis of palladium and platinum nanoparticles immobilized in pores of mesoporous aromatic frameworks, which represent a new class of carbon supports with a diamond-like ordered structure. The resulting materials have been characterized by transmission electron microscopy, IR spectroscopy, and NMR spectroscopy. It has been shown that the catalyst activity in the hydrogenation reaction depends on the substrate molecule size and adsorbability on the surface of nanoparticles. Catalytic activity has been studied in the hydrogenation of a number of unsaturated compounds at temperatures of 60 and 80°C and pressures of 1.0 and 3.0 MPa.

Keywords: nanoparticles, catalysis, mesoporous materials, hydrogenation

DOI: 10.1134/S0965544117020177

One of the most important processes in the modern petrochemical industry is the hydrogenation of unsaturated compounds. This process is commonly used to improve the characteristics of motor fuels by removing polyunsaturated compounds and olefins from the gasoline and diesel fractions, remove adverse undesirable compounds—acetylenes and dienes—from pyrolysis products, and produce cyclohexane and cyclohexanol, which are key intermediates in the synthesis of adipic acid and caprolactam [1–3]. An increasingly significant role is played by the selective hydrogenation of benzene to cyclohexene, which has already been implemented in industry [4]. In this context, the design of novel catalyst systems exhibiting high activity and selectivity in the hydrogenation of a broad range of unsaturated compounds is an urgent and important problem.

At present, one of the rapidly developing fields of catalysis is the use of mesoporous polymer supports for the stabilization of metal nanoparticles and the design of catalysts for various petrochemical processes [5–8]. Materials of this type include porous aromatic frameworks (PAFs), which represent a novel class of carbon materials with an ordered regular structure (see below). The main advantages of this material are high chemical and thermal stability, simple methods of structure functionalization, and the possibility of imposing an average pore size in the synthesis of these materials [9–11]. Furthermore, the aromatic nature of the supports contributes to a better diffusion of

organic substrates deep into the pores of the material than that in the case of conventional inorganic supports; the structural features of mesoporous aromatic supports provide a narrow size distribution of metal nanoparticles and their better stabilization compared with classical carbon supports. All these features make PAFs an attractive type of supports for designing metal-containing catalysts.

The use of mesoporous aromatic frameworks for synthesizing hydrogenation catalysts based on ruthenium nanoparticles stabilized by the pores of the material was previously reported in [12]. The resulting catalysts were active in the exhaustive hydrogenation of a broad range of aromatic substrates; in addition, it was shown that a variation in the pore size in the starting material makes it possible to adjust the average size of the resulting metal particles and affect the substrate selectivity of the catalyst.

This study is focused on the synthesis of platinum and palladium nanoparticles inside the pores of mesoporous aromatic frameworks and examination of the activity of the synthesized catalysts in the hydrogenation of unsaturated compounds.

EXPERIMENTAL

Precursors

The following materials were used as substrates: styrene (Arcos Organics, 97%); α -methylstyrene

Table 1. Gas–liquid chromatography analysis conditions

Carrier gas	Nitrogen ($P = 200$ kPa), volume flow rate of 30 mL/min		
groups of substrates	styrene, methylstyrene, phenylacetylene, decene, toluene	octene, octyne, dimethylhexadiene	benzene
Detector temperature, °C	250		
Injector temperature, °C	250		
Initial column temperature, °C	60	60	35
Final column temperature, °C	220	220	35
Column heating rate, °C/min	10	10	0
Initial time, min	10	5	20
Final time, min	5	10	1

(Aldrich, 99%); phenylacetylene (Aldrich, 98%); octene-1 (Aldrich, 98%); octyne-4 (Aldrich, 99%); 2,5-dimethylhexadiene-2,4 (Aldrich, 96%); decene-1 (Arcos Organics, 95%); benzene (Irea 2000, analytical grade); toluene (Khimmed, special purity grade); and ethylbenzene (Reakhim, high-purity grade). Methanol (Acros Organics, 99+%); ethanol (Irea 2000, analytical grade); and chloroform (Khimmed, high-purity grade) were used as solvents.

The solvents were purified according to standard procedures. PAF-30 was synthesized as previously described in [12]. To deposit metals into the framework pores, the supports were impregnated with metal salts, which were subsequently reduced with an alcoholic solution of sodium borohydride. Metal sources were palladium(II) acetate (Aldrich, 99.9%) and a 1% aqueous solution of hexachloroplatinic(IV) acid to synthesize palladium and platinum catalysts, respectively.

Instruments and Investigation Procedures

IR spectroscopy. IR spectra of the synthesized samples were recorded in a range of 4000–400 cm^{-1} on a Nicolet IR-2000 instrument (Thermo Scientific) by the multiple attenuated total internal reflection method using a Multi-reflection HATR accessory comprising a 45° ZnSe crystal for different wavelength ranges with a resolution of 4 nm.

Solid-state NMR spectroscopy. Analysis by polarization-transfer solid-state ^{13}C NMR spectroscopy (CPMAS) was conducted on a Varian NMR Systems instrument at an operating frequency of 125 MHz in a pulse mode at a rotation frequency of 10 kHz.

Low-temperature nitrogen adsorption. Nitrogen adsorption/desorption isotherms were recorded at a temperature of 77 K on a Micromeritics Gemini VII 2390 (V1.02t) instrument. Before measurements, the samples were degassed at a temperature of 110°C for 6 h. The surface area (S_{BET}) was calculated by the Brunauer–Emmett–Teller (BET) method on the basis of adsorption data in a range of relative pressures

(P/P_0) of 0.05–0.2. Pore volume and pore size distribution were determined from the adsorption branch of the isotherm using the Barrett–Joyner–Halenda (BJH) model. Total pore volume (V_{tot}) was determined from the amount of nitrogen adsorbed at a relative pressure of $P/P_0 = 0.995$.

Transmission electron microscopy (TEM). Analysis of materials by TEM was conducted on a LEO912c AB OMEGA instrument (magnification of 80× to 500000×; image resolution of 0.2–0.34 nm). The electron beam potential was 100 eV. The processing of the micrographs and the calculation of the average particle size were conducted using the ImageJ software program.

Atomic emission spectroscopy. The quantitative determination of palladium and platinum in the samples was conducted by inductively coupled plasma atomic emission spectroscopy on an IRIS Interpid II XPL instrument (Thermo Electron Corp., United States) with radial and axial viewing at wavelengths of 310 and 95.5 nm.

Gas–liquid chromatography. Analysis of the reaction products was conducted on a ChromPack CP9001 chromatograph equipped with a flame ionization detector and a 30 m × 0.2 mm column (SE-30 grafted phase) using nitrogen as a carrier gas at a flow rate of 30 mL/min. Chromatograms were recorded and analyzed on a computer using the Maestro 1.4 software program. Conversion was determined from changes in the relative peak areas of the substrate and the products (in %). The analysis conditions are given in Table 1.

Catalyst Synthesis Procedure

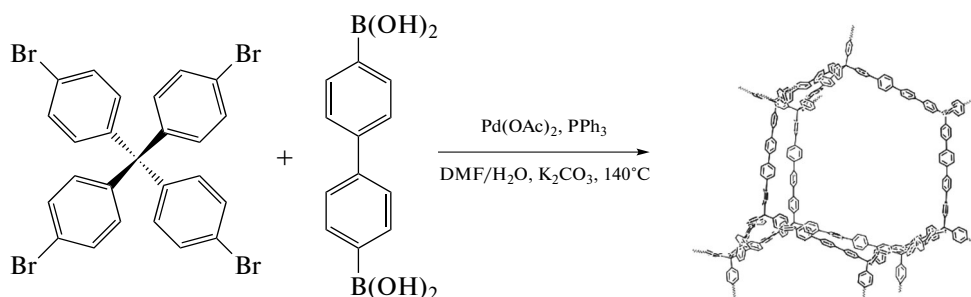
Catalysts were synthesized by impregnating the support material with solutions of metal salts, which were subsequently reduced with a methanolic solution of sodium borohydride. To this end, a 0.01 M solution of palladium(II) acetate in chloroform was used in the case of the PAF-30–Pd palladium catalyst; an aqueous methanol solution of hexachloroplatinic(IV) acid,

which was prepared in a ratio of 5 mL of a 1% aqueous $\text{H}_2[\text{PtCl}_6]$ solution per 20 mL of methanol, was employed for the PAF-30–Pt platinum catalyst. In both catalysts, the calculated amount of the metal was 5 wt %.

A typical procedure includes the drying of 400 mg of the original PAF-30 support in a vacuum at 60°C for 1 h and the subsequent impregnation of it with 20 mL of a palladium acetate solution in chloroform in a round-bottom flask equipped with a magnetic stirrer anchor and a reflux condenser at room temperature under continuous stirring for 12 h. After this time, 40 mL of a freshly prepared 0.33 M solution of sodium borohydride in methanol was dropwise added to the resulting suspension. The resulting catalyst was isolated by filtration; to remove the sodium borate formed as a reaction product, the precipitate was washed with water and alcohol several times. In either case, after drying in a vacuum, the resulting products had the form of a dark gray powder.

Catalytic Testing Procedure

According to a typical procedure, a calculated amount of a catalyst and a substrate were placed in a temperature-controlled steel autoclave equipped with a test-tube liner and a magnetic stirrer anchor; all catalytic reactions were run without using any solvent. The autoclave was sealed, filled with hydrogen to a pressure of 10 or 30 atm, and connected to a thermostat. The reaction was run under vigorous stirring at 60°C for 15, 30, or 60 min; after that, the autoclave was cooled below room temperature and depressurized.



Scheme 1. Schematic synthesis of mesoporous aromatic framework PAF-30.

The resulting material was characterized by IR spectroscopy, solid state NMR spectroscopy, and low-temperature nitrogen adsorption–desorption. The IR spectrum of the material exhibits a strong absorption band peaking at 808 cm^{-1} , which corresponds to the δ_{oop} vibrations of the C–H bond, and less intense absorption bands $\nu\text{ C}=\text{C}_{\text{p-Ar}}$ and $\delta_{\text{ip}}\text{ C}_{\text{sp}^3}\text{--C}_{\text{Ar}}$ peaking at 1485 and 1004 cm^{-1} , respectively. It should be noted that no absorption bands characteristic of vibrations of the B–OH and C–Br bonds are observed in regions of

Catalyst activity for each reaction was calculated according to the following formula:

$$\text{TOFs} = \frac{\text{Conv} \times n(\text{Sub})}{\Delta t \times n(\text{Me}) D},$$

where Conv is the conversion of the substrate to the product, %; $n(\text{Sub})$ is the substrate content, mol; Δt is the reaction time, h; $n(\text{Me})$ is the total metal content, mol; and D is the metal dispersion, which determines the ratio between the number of surface atoms and the number of atoms in the bulk of the particle; it is calculated as follows:

$$D = \frac{6V_A}{S_A \times d_{\text{pt}}} = \frac{6V_M(\text{Me}) \times k}{N_A \times S_A \times d_{\text{pt}}} = \frac{X}{d_{\text{pt}}},$$

where d_{pt} is the average metal particle size, Å; V_A is the atomic volume of the metal phase; S_A is the normalized landing pad area on the particle surface; $V_M(\text{Me})$ is the molar volume of the metal; k is the crystal structure packing factor; N_A is the Avogadro's number; and X is the coefficient derived after simplification of the formula for calculating the metal dispersion by the substitution of known constants; for palladium and platinum, $X \sim 8.85$ and 11.12 , respectively [13].

RESULTS AND DISCUSSION

Characterization of PAF-30

Mesoporous aromatic framework PAF-30 was synthesized of tetrakis[*p*-bromophenyl]methane and 4,4'-biphenyldiboric acid by the Suzuki cross-coupling reaction as previously described in [12] (Scheme 1).

$3100\text{--}3600$ and 1076 cm^{-1} ; this fact confirms the completeness of the cross-coupling reaction.

The ^{13}C NMR spectrum of the material exhibits signals characteristic of sp^2 -hybridized carbon atoms of aromatic moieties in the region of $120\text{--}150$ ppm and a low-intensity signal at 68 ppm corresponding to sp^3 -hybridized carbon atoms in the nodes of tetraphenylmethane moieties. Similar to the IR spectroscopy data, the spectrum of the synthesized framework

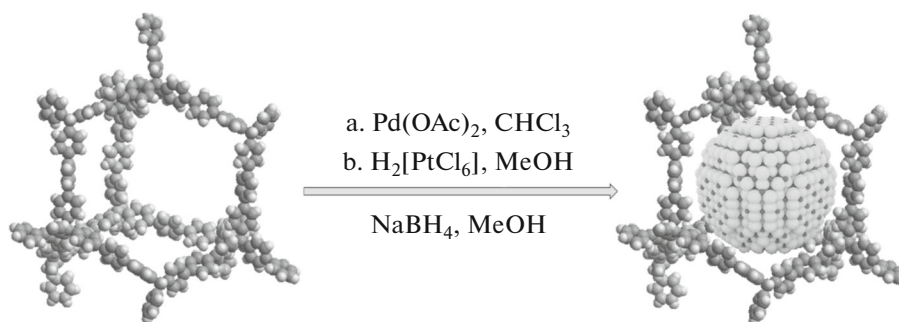
does not exhibit a C_{Ar-Br} signal (120.0 ppm) characteristic of tetrakis[*p*-bromophenyl]methane.

The low-temperature nitrogen adsorption–desorption studies of the porosity of the synthesized aromatic frameworks revealed an abrupt absorption of nitrogen at low pressures ($P/P_0 = 0–0.05$), which indicates the presence of micropores in the material structure. In addition, in a relative pressure range of $P/P_0 = 0.2–0.9$, the nitrogen adsorption curve gradually ascends without exhibiting a plateau; in addition, a characteristic hysteresis loop between the adsorption and desorption curves is observed; these findings confirm the mesoporous nature of the resulting frame-

works. The synthesized polymer frameworks are characterized by lower average specific surface area ($S_{BET} = 382 \text{ m}^2/\text{g}$) and pore volume ($V_p = 0.17 \text{ cm}^3/\text{g}$) compared with the previously reported values [14, 15] and an average pore size of 3.5 nm.

Characterization of the Catalysts

Both the PAF-30–Pd and PAF-30–Pt catalysts synthesized by the immobilization of metal nanoparticles in the support pores contained 5 wt % of the metal (Scheme 2). The resulting materials were characterized by atomic emission spectroscopy and TEM.



Scheme 2. Immobilization of metal nanoparticles inside the framework pores.

Figure 1 shows micrographs of the catalysts, the particle size distribution, and the metal content in the resulting materials. It should be noted that, in the case of the PAF-30–Pt catalyst, the particle size distribution curve exhibits several local minima at 3.5 and 7.0 nm and a maximum at 5.3 nm, while the particle size distribution for the PAF-30–Pd catalyst is close to normal (Gaussian) and exhibits a maximum at 3.2 nm.

In addition, the platinum catalyst is characterized by the formation of large agglomerates of particles located mostly on the surface. This finding can be attributed to the ionic nature of the salt and, as a consequence, hindrances to the diffusion of the $[PtCl_6]^{2-}$ into the pores of the material.

In the case of the palladium catalyst, the lower average metal particle size is apparently attributed to the absence of dissociation of palladium acetate in a chloroform solution and the existence of the salt in the form of a cyclic trimer and a linear dimer [16]; this feature provides a more uniform distribution of the salt over the support volume.

Catalytic Tests

The synthesized materials were tested as catalysts for the hydrogenation of a series of unsaturated compounds. It was previously shown that Pd and Pt nanoparticles supported on mesoporous phenol formaldehyde resins are active in the selective hydrogenation

of alkynes and dienes to olefins [17, 18]. The main results are shown in Fig. 2 and Table 2.

In all cases, the activity of the platinum-based PAF-30–Pt catalyst was significantly higher than that of the palladium-based PAF-30–Pd catalyst, while the selectivity for products of incomplete hydrogenation of substrates with multiple unsaturated bonds (phenylacetylene, 2,5-dimethylhexadiene-2,4) was exhibited by the PAF-30–Pd palladium catalyst. The catalytic test results are consistent with the literature data, according to which platinum-containing catalysts exhibit higher activity and lower selectivity than those of palladium-based catalysts [19, 20].

The hydrogenation ability of the catalysts correlates with the substrate molecule sizes and adsorbability. Thus, the catalyst activity decreases with increasing number of carbon atoms in the substrate molecule; this finding is attributed to diffusion limitations during the passage of the substrate through the framework pores. The presence of a benzene ring in the substrate structure contributes to the diffusion inside mesoporous aromatic frameworks owing to π – π stacking interactions with the support material and facilitates the adsorption of the substrate on the metal particle surface. Thus, in the case of the PAF-30–Pt catalyst, the complete conversion of styrene to ethylbenzene is achieved within 30 min, while the catalyst activity, which is expressed in terms of the turnover number per unit time per number of metal atoms on the particle surface, is highest in the case of

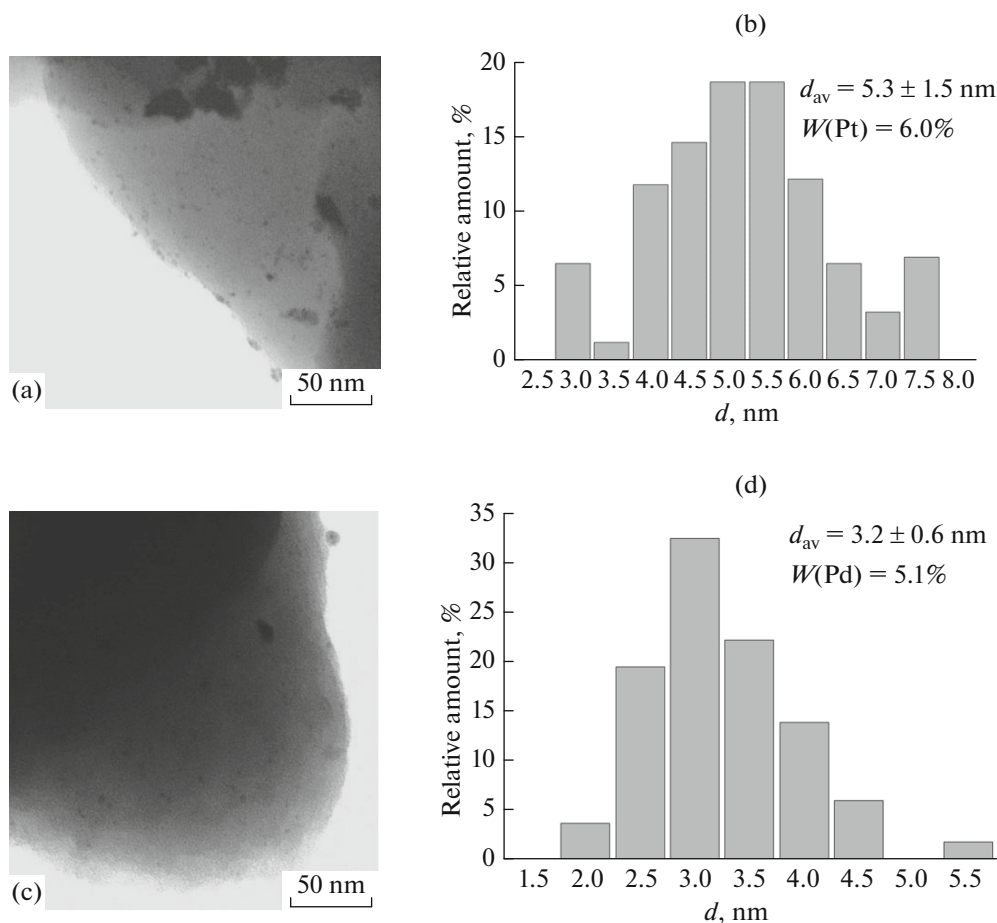


Fig. 1. Micrographs of the catalysts and metal particle size distribution for (a, b) the PAF-30-Pt and (c, d) PAF-30-Pd materials.

styrene; the factors responsible for this feature include an increase in the electron density of the C=C double bond owing to the conjugation of the bond with the aromatic ring [21, 22].

The reuse of the synthesized catalysts was studied using the example of hydrogenation of octene-1. In either case, a slight decrease in the catalyst activity was observed; this finding is mostly associated with the catalyst losses during decantation. After six hydrogenation runs, the octene-1 conversion was 64 and 28% in the case of the platinum-based PAF-30-Pt and palladium-based PAF-30-Pd catalysts, respectively. Thus, the synthesized catalysts can be reused without any significant loss of activity.

The PAF-30-Pt platinum catalyst was tested in the hydrogenation of aromatic compounds (Fig. 3). The main products of the reaction were appropriate cyclohexane derivatives. Similar to the previous results, the hydrogenation product yield decreases with increasing substrate molecule size. It should be noted that this relationship exhibits an inverse linear behavior; this finding is consistent with the data derived for ruthenium-containing catalysts [12].

The activity of the synthesized catalysts was compared with the activity of previously described catalysts (Tables 3, 4). To determine the activity of the

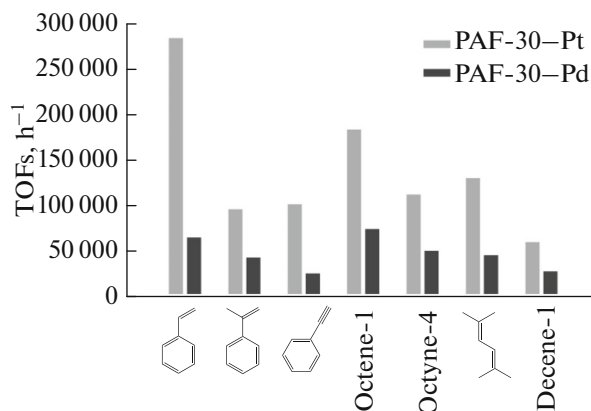
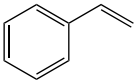
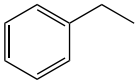
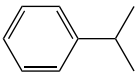
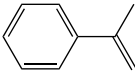
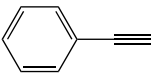
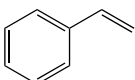
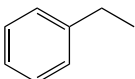
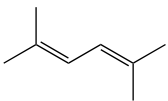
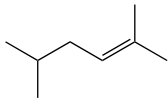
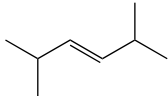
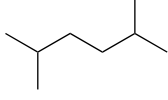


Fig. 2. Hydrogenation of unsaturated substrates over the PAF-30-Pd and PAF-30-Pt catalysts. Reaction conditions: 1 mg of the catalyst; substrate : metal = 27000 : 1 (mol); 1 MPa H_2 ; 60°C; and 30 min (styrene, 15 min; methylstyrene, 60 min).

Table 2. Distribution of unsaturated compound hydrogenation products in the presence of the PAF-30–Pd and PAF-30–Pt catalysts. Reaction conditions are given in the caption to Fig. 2

Substrate	Reaction products	Product yield, %	
		PAF-30–Pd	PAF-30–Pt
		22	55
		44	75
		13	33.5
		0.2	3
Octene-1	octane	38	71
	<i>trans</i> -octene-2	33.6	8
	<i>cis</i> -octene-2	20	2
	<i>trans</i> -octene-4	1	1
	other octenes	4.5	3
Octyne-4	<i>cis</i> -octene-4	24	40
	<i>trans</i> -octene-4	0.5	0.8
	octane	0.2	0.2
		7	2
		14.5	8
		1	20
Decene-1	Decane	14	23
	Products of decene-1 isomerization via double bond migration	82	68

PAF-30–Pd and PAF-30–Pt catalysts in the hydrogenation reaction, styrene and phenylacetylene, respectively, were selected as a substrate. The tables show that the catalysts are highly active in the hydrogenation of the selected substrates.

Thus, it has been found that the synthesized catalysts exhibit high activity and stability in the hydrogenation of a series of unsaturated compounds. Higher activity is observed for the platinum-based PAF-30–Pt catalyst, while higher selectivity for

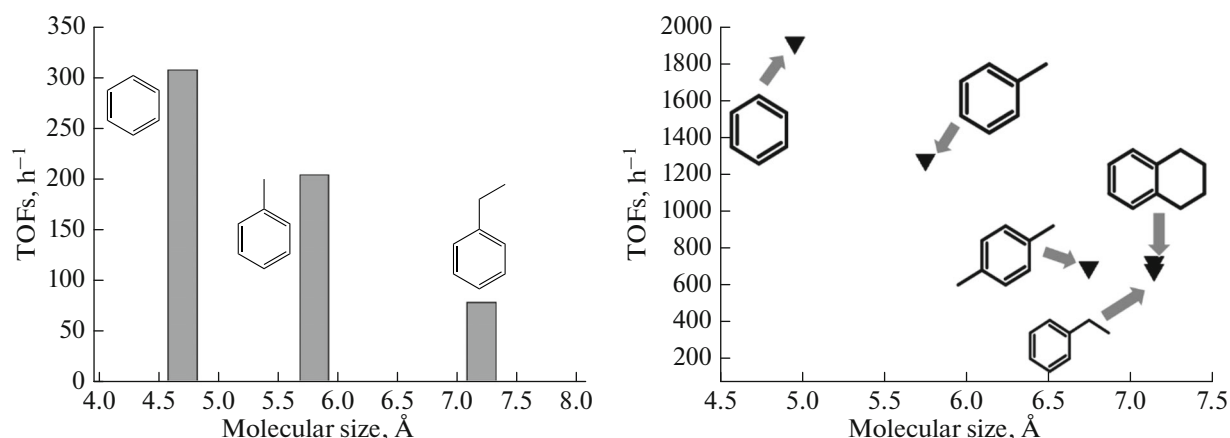


Fig. 3. Dependence of the catalyst activity on the substrate molecule size: PAF-30-Pt (left) and PAF-30-Ru (right, plotted according to the data of [12]). Reaction conditions: 24 mg of the PAF-30-Pt catalyst; substrate : metal = 1500 : 1 (mol); 3 MPa H₂; 80°C; and 6 h.

Table 3. Comparison of the activity of the PAF-30-Pd catalyst with the activity of other Pd-containing catalysts using the example of styrene hydrogenation. In all cases, the only reaction product was ethylbenzene

Catalyst	Reaction conditions	Styrene conversion, %	TOF, h ⁻¹	Source
PAF-30-Pd (5.1% Pd)	1 mg of catalyst, 1.4 mL of styrene, 1 MPa H ₂ , 60°C, 15 min	22%	23760	This study
PPI-BP-1-Pd (2) (7.61% Pd)	0.95 mg of catalyst, 1 mL of styrene, 1.5 mL of benzene, 1 MPa H ₂ , 70°C, 15 min	67%	34440	[21]
Pd/C* (3% Pd)	5 mg of catalyst, 1 μL of styrene (0.115 mL), 15 mL of methanol, 0.1 MPa H ₂ , 25°C	n/a*	2730	[23]
Pd-Al ₂ O ₃ (0.3% Pd)	10 g of catalyst, 31 mL of styrene, 370 mL of heptane, 3 MPa H ₂ , 40°C, 10 min	44%	2790	[24]

* The study provides data on the hydrogenation reaction rate in the linear portion of the time dependence of the product concentration.

Table 4. Comparison of the activity of the PAF-30-Pt catalyst with the activity of other Pt-containing catalysts using the example of phenylacetylene hydrogenation

Catalyst	Reaction conditions	Substrate conversion, %	Styrene selectivity, %	TOF, h ⁻¹	Source
PAF-30-Pt (6.0% Pt)	1 mg of catalyst, 1.4 mL of substrate, 1 MPa H ₂ , 60°C, 15 min	36.5	92	42570	This study
MPF-SO ₃ H-Pt (c) (0.2% Pt)	1 mg of catalyst, 1 mL of substrate, 1.5 mL of benzene, 1 MPa H ₂ , 80°C, 15 min	43	89	55800	[18]
Pt/C (5% Pt)	0.3 g of catalyst, 2.6 mL of substrate, 35 mL of ethanol, 1 MPa H ₂ , 20°C, 10 min	67	78	1510	[25]
Pt-Al ₂ O ₃ (0.5% Pt)	150 mg of catalyst, 1 mL of substrate (C = 0.042 M), 200 mL of tetradecane, 0.38 MPa H ₂ , 75°C, 12 min	62	77	9030	[26]

incomplete hydrogenation products is obtained using the PAF-30–Pd catalyst. Using the example of the platinum-based PAF-30–Pt catalyst, it has been shown that the catalyst activity exhibits an inverse linear dependence on the substrate molecule size in the exhaustive hydrogenation of aromatic hydrocarbons.

ACKNOWLEDGMENTS

This work was supported by a grant of the Russian Science Foundation, project no. 15-19-00099.

REFERENCES

1. A. B. Kulikov, A. A. Pugacheva, and A. L. Maksimov, *Pet. Chem.* **54**, 426 (2014).
2. A. Maximov, A. Zolotukhina, V. Murzin, et al., *Chem. Cat. Chem.* **7**, 1197 (2015).
3. E. A. Karakhanov, A. G. Dedov, L. E. Tskhai, and V. V. Shatalov, *Pet. Chem.* **33**, 202 (1993).
4. H. Ishida, *Catal. Surv. Asia* **1**, 241 (1997).
5. A. Taguchi and F. Schuth, *Micropor. Mesopor. Mater.* **77**, 1 (2005).
6. C. Perego and R. Millini, *Chem. Soc. Rev.* **42**, 3956 (2013).
7. E. Karakhanov, Yu. Kardasheva, L. Kulikov, et al., *Catalysts* **6** (8), 122 (2016).
8. S. V. Lysenko, I. O. Kryukov, O. A. Sarkisov, et al., *Pet. Chem.* **51**, 202 (2011).
9. E. Merino, E. Verde-Sesto, E. M. Maya, et al., *Appl. Catal., A* **469**, 206 (2014).
10. T. Ben, H. Ren, S. Ma, et al., *Angew. Chem., Int. Ed. Engl.* **48**, 9457 (2009).
11. J. R. Holst, E. Stockel, D. J. Adams, and A. I. Cooper, *Macromolecules* **43**, 8531 (2010).
12. A. Maximov, A. Zolotukhina, L. Kulikov, Yu. Kardasheva, E. Karakhanov, *React. Kinet. Mech. Catal.* **117**, 729 (2016).
13. J. Anderson, *Structure of Metallic Catalysts* (Academic, London, 1975).
14. Y. Yuan, F. Sun, H. Ren, et al., *J. Mater. Chem.* **21**, 13498 (2011).
15. M. Rose, N. Klein, W. Bohlmann, et al., *Soft Matter* **6**, 3918 (2010).
16. E. S. Stoyanov, *Zh. Strukt. Khim.* **41**, 540 (2000).
17. E. A. Karakhanov, A. L. Maksimov, I. A. Aksenov, et al., *Russ. Chem. Bull.* **63**, 1710 (2014).
18. M. P. Boronoev, E. S. Subbotina, A. A. Kurmaeva, et al., *Pet. Chem.* **56**, 109 (2016).
19. G. Carturan, G. Cocco, G. Facchin, and G. Navazio, *J. Mol. Catal.* **26**, 375 (1984).
20. A. K. Talukdar and K. G. Bhattacharyya, *Appl. Catal., A* **96**, 229 (1993).
21. E. Karakhanov, A. Maximov, Yu. Kardasheva, et al., *ACS Appl. Mater. Interfaces* **6**, 8807 (2014).
22. S. D. Jackson, H. Hardy, G. J. Kelly, and L. A. Shaw, *Stud. Surf. Sci. Catal.* **108**, 305 (1997).
23. P. Kacer and L. Cerveny, *J. Mol. Catal. A* **212**, 183 (2004).
24. Z. Zhou, Z. Cheng, Y. Cao, et al., *Chem. Eng. Technol.* **30**, 105 (2007).
25. F. B. Bizhanov, S. D. Dinasylova, and D. V. Sokolskii, *React. Kinet. Catal. Lett.* **12**, 291 (1979).
26. B. A. Wilhite, M. J. McCreedy, and A. Varma, *Ind. Eng. Chem. Res.* **41**, 3345 (2002).

Translated by M. Timoshinina